

Conformational Control in Dirhodium(II) Paddlewheel Catalysts Supported by Chalcogen-Bonding Interactions for Stereoselective Intramolecular C–H Insertion Reactions

Takuya Murai, Wenjie Lu, Toshifumi Kuribayashi, Kazuhiro Morisaki, Yoshihiro Ueda, Shohei Hamada, Yusuke Kobayashi, Takahiro Sasamori, Norihiro Tokitoh, Takeo Kawabata, and Takumi Furuta*



Cite This: *ACS Catal.* 2021, 11, 568–578



Read Online

ACCESS |



Metrics & More



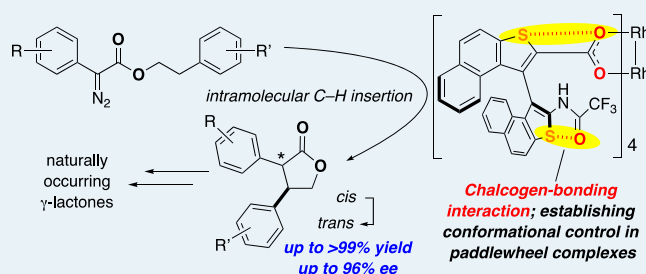
Article Recommendations



Supporting Information

ABSTRACT: D_2 -symmetric dirhodium(II) carboxylate catalysts that bear axially chiral binaphthothiophene δ -amino acid derivatives have been developed. Conformational control is supported through chalcogen-bonding interactions between sulfur and oxygen atoms in each ligand, providing well-defined and uniform asymmetric environments around the catalytically active Rh(II) centers. These structural properties make such complexes asymmetric catalysts for the stereoselective intramolecular C–H insertion into α -aryl- α -diazoacetates to yield a variety of *cis*- α,β -diaryl γ -lactones, as well as the corresponding *trans*-isomers through epimerization, in high diastereo- and enantioselectivities. Short total syntheses of the naturally occurring γ -lactones, cinnamomumolide, cinnassin A₇, and cinnamomulactone were also accomplished using this conformationally controlled catalyst.

KEYWORDS: paddlewheel complex, chalcogen bond, intramolecular C–H insertion, axially chiral amino acid, γ -Lactone



INTRODUCTION

Chiral dirhodium(II) paddlewheel complexes are highly valuable catalysts for stereoselective transformations including insertion reactions in X–H bonds (X = C, N, O, etc.) (Figure 1A) as well as the stereoselective cyclopropanation of unsaturated C=C bonds through the decomposition of diazo compounds.¹ Some of the most frequently employed chiral dirhodium(II) paddlewheel catalysts are dirhodium(II) carboxylate complexes that bear chiral carboxylate groups as paddlewheel ligands.

The construction of a defined asymmetric environment around the catalytically active center is crucial for the development of potential asymmetric catalysts. However, the construction of defined asymmetric environments can be very difficult, especially in the case of catalysts with rotatable bonds near the catalytically active center. Dirhodium(II) carboxylate complexes represent typical examples of catalysts that suffer from undesirable conformational flexibility around the rotatable C–C bond of the carboxylate groups tethered to Rh(II) (Figure 1B). Their conformational flexibility often complicates the construction of defined chiral environments around the upper (Rh1) and lower (Rh2) rhodium atoms, both of which act as catalytically active centers; however, it also enables the construction of diverse and interchangeable structures with different molecular symmetries. Specifically, C_1 -, C_2 -, C_4 -, and D_2 -symmetric structures with up-up-down-down, up-up-down-down, all-up, and up-down-up-down ligand

arrangements relative to the plane of the rhodium carboxylate moieties, respectively, can be formed (Figure 1B).² The presence of uniform chiral environments around the Rh1 and Rh2 centers is particularly important in C_2 (up-up-down-down)- and D_2 (up-down-up-down)-symmetric catalysts, as inequivalent chiral environments will produce products with nonuniform optical purity. Therefore, an important issue in the development of potential dirhodium(II) carboxylate catalysts is establishing control over the conformational flexibility of the carboxylate ligands around the C–C single bond.

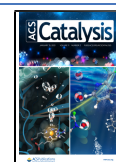
We envisioned that the introduction of an interaction that fixes one conformation of the rotatable carboxylate C–C bond could provide a dirhodium(II) complex with relatively rigid and uniform chiral environments around the Rh1 and Rh2 centers.

We have previously reported the synthesis of axially chiral binaphthyl δ -amino acid (*S*)-1 and its *N*-protected derivatives (Figure 1C),³ as well as their application as chiral carboxylate ligands in dirhodium(II) carboxylate catalyst 2a (Figure 2B).⁴ Later, we extended these studies to prepare the binaphtho-

Received: August 24, 2020

Revised: December 9, 2020

Published: December 28, 2020



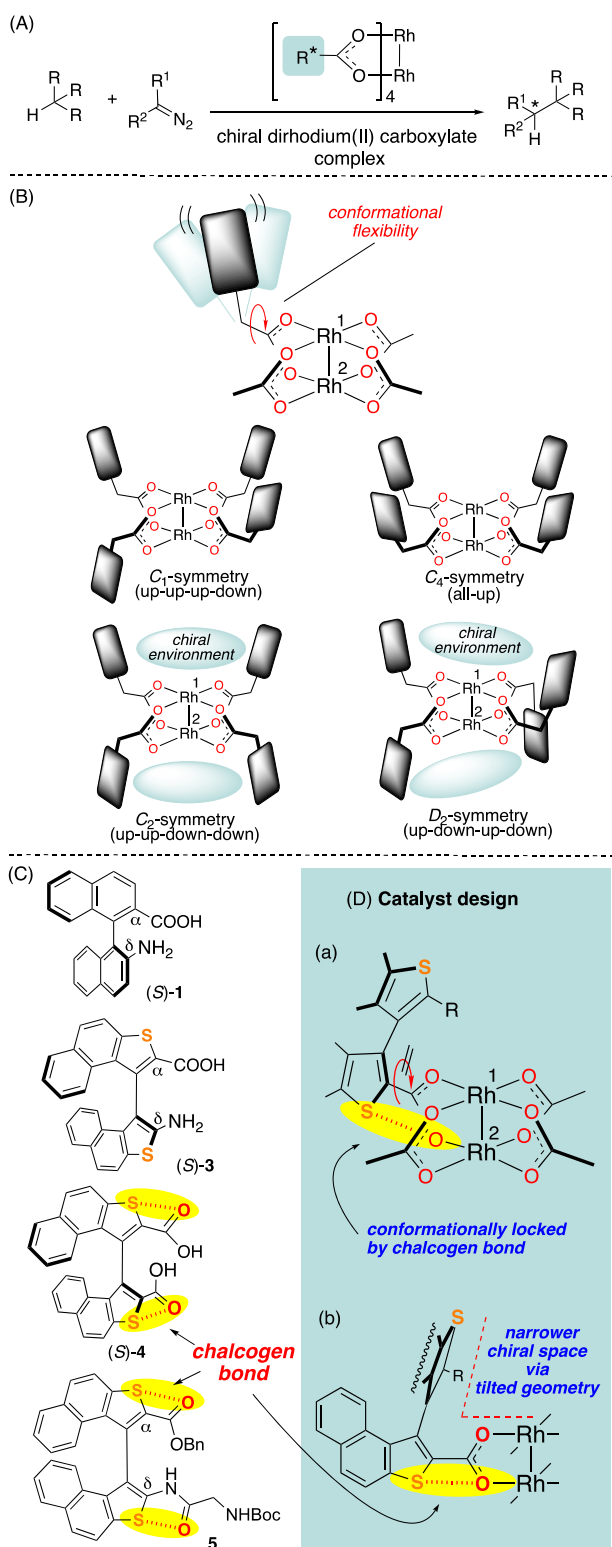
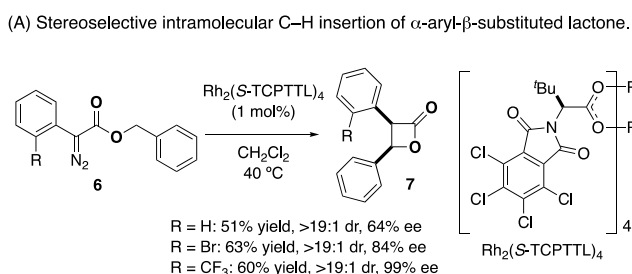
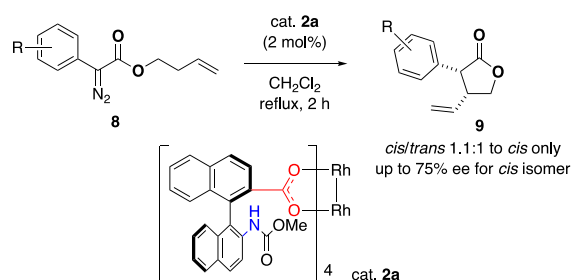


Figure 1. (A) C–X bond insertion reaction catalyzed by a dirhodium(II) carboxylate complex. (B) Conformational flexibility and ligand arrangement in dirhodium(II) carboxylate complexes. (C) Axially chiral binaphthyl and binaphthothiophene δ -amino acids and their chalcogen-bond-containing derivatives. (D) Schematic illustration of the concept for the design of the catalyst used in this study.

thiophene δ -amino acid (S)-3, which contains sulfur atoms in its fused π -system, from binaphthothiophene dicarboxylic acid (S)-4 (Figure 1C).^{5,6} Furthermore, racemic 3 was transformed



(B) Our example of stereoselective intramolecular C–H insertion.



(C) This work

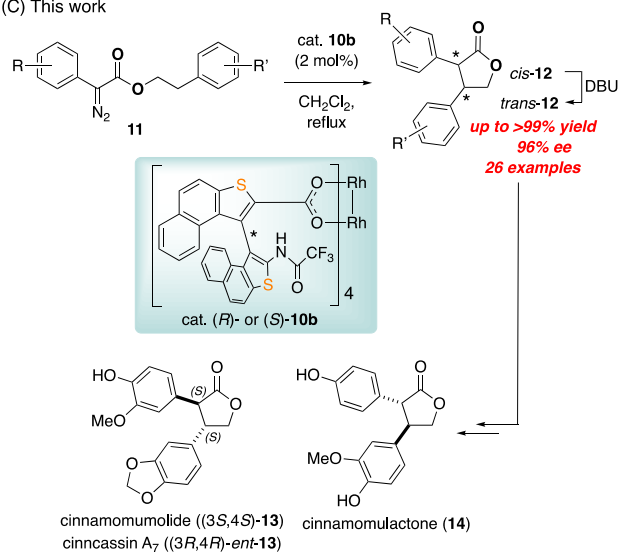


Figure 2. Stereoselective intramolecular C–H insertion reactions of α -aryl α -diazoesters catalyzed by dirhodium(II) carboxylate complexes.

into the corresponding amide derivative 5.⁶ Single-crystal X-ray diffraction analyses of (S)-4 and 5 revealed chalcogen bonds (S \cdots O interactions) between the oxygen atom of the carbonyl group and the sulfur atom of the naphthothiophene ring, which resulted in a coplanar conformation.

Chalcogen bonding has been recognized as a noncovalent interaction that plays a role in determining the conformation of pharmaceuticals and organic materials.⁷ Recently, this interaction has also received attention as a driving force in organocatalysis⁸ as well as an attractive interaction in supramolecular assembly.⁹ We envisaged that the chalcogen-bonding interactions found in (S)-4 and 5 could be used to lock the conformation of the carboxylate C–C bonds to fix the stereostructure of dirhodium(II) complexes (Figure 1D(a)).¹⁰ Furthermore, this conformational restriction would result in a tilt of the other aromatic ring system of the biaryl ligand toward the inside of the complex to give a narrow and well-

defined chiral space near the catalytically active Rh centers (Figure 1D(b)). Such chiral environments can be expected to result in good asymmetric induction.

Asymmetric intramolecular C–H insertion of α -diazoacetates has been investigated as a powerful synthetic tool for constructing a variety of chiral cyclic compounds. Although a variety of stereoselective intramolecular C–H insertions have been reported,¹¹ some of the reactions are still retained to achieve high stereoselectivity. The stereoselective intramolecular C–H insertion of α -aryl- α -diazoesters into α -aryl- β -substituted lactones is one of the examples of the reactions that are still difficult to access.^{12,13} As an exceptional example, the highly enantio- and diastereoselective C–H insertion reaction of **6** to give α,β -diaryl β -lactone **7** has been reported by Davies and co-workers; however, a trifluoromethyl or halogen group at the *ortho*-position of the α -aryl group was required to ensure satisfactory levels of stereoselectivity (Figure 2A).¹³ We have also examined the stereoselective C–H insertion reaction of 3-butenyl α -aryl- α -diazoacetates **8** catalyzed by **2a** to give α -aryl- β -substituted γ -lactones **9** (Figure 2B).⁴ However, the obtained levels of enantio- and diastereoselectivity were unsatisfactory.

We envisioned that catalysts that are conformationally locked via chalcogen-bonding interactions could potentially provide a solution for these problematic intramolecular C–H insertion reactions.

Even though the initial attempts using **2a** were unsatisfactory (Figure 2B), the asymmetric construction of α -aryl β -substituted γ -lactones continued to attract us because this type of lactone is frequently found as the core structure of natural products¹⁴ such as cinnamomumolide (**13**),¹⁵ cinnocassin A₇ (*ent*-**13**),¹⁶ and cinnamomulactone (**14**)¹⁷ (Figure 2C). Therefore, we developed in this study a novel type of dirhodium(II) carboxylate catalyst and revealed that **10b**, whose conformation can be controlled via chalcogen-bonding interactions, is a highly valuable catalyst for intramolecular C–H insertion reactions.

Herein, we report the stereostructures of the sulfur-containing catalyst **10b** and related derivatives, together with its successful application in the stereoselective C–H insertion of **11** to give α,β -diaryl γ -lactones **12**, as well as its extension to the total syntheses of **13**, *ent*-**13**, and **14** (Figure 2C).

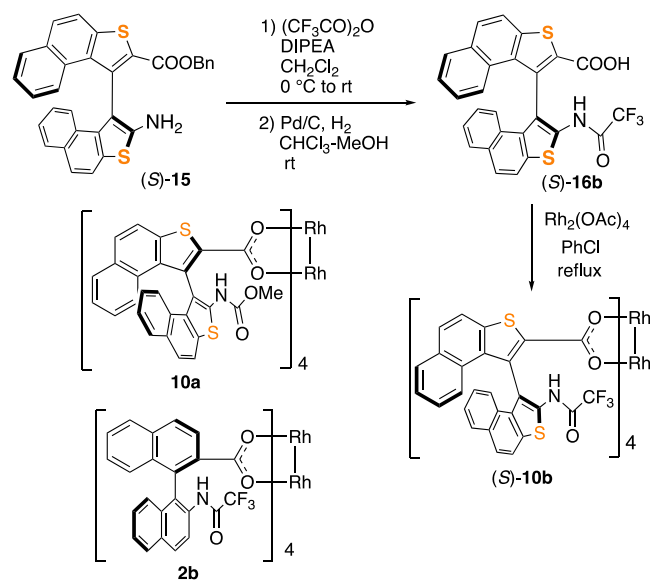
RESULTS AND DISCUSSION

Preparation and Stereostructure of Dirhodium(II) Carboxylate Complexes. Complex (*S*)-**10b**, which bears a trifluoroacetamide group on its binaphthothiophene framework, was prepared from benzyl ester (*S*)-**15**⁶ by installing a trifluoroacetamide moiety at the aniline-type amino group and successive deprotection of the benzyl group (Scheme 1). Treatment of carboxylic acid (*S*)-**16b** with Rh₂(OAc)₄ in refluxing chlorobenzene led to a smooth ligand exchange from AcOH to (*S*)-**16b** on the rhodium(II) centers to afford (*S*)-**10b**. We also prepared enantiomer (*R*)-**10b**, the methoxycarbonyl-functionalized analogue **10a**, and the binaphthyl-type **2b**, which contains trifluoroacetamide groups, to compare their catalytic potential to that of **10b**.

The success of the catalyst-design concept presented in Figure 1D was confirmed by single-crystal X-ray diffraction analyses of (*S*)-**10b** and **2b**. The crystal structure of **2b** is shown in Figure 3A.

In the crystalline solid state, **2b** adopts a D₂-symmetric conformation in which the amide-substituted naphthyl groups reside in an “up-down-up-down” conformation.^{18,19} However,

Scheme 1. Preparation of Biaryl-Type Dirhodium(II) Carboxylate Complexes **2b**, **10a**, and (*S*)-**10b**



the structure of **2b** was found to be pseudosymmetric, i.e., the chiral environments around the two rhodium centers (Rh1 and Rh2) are not identical, as indicated by the different geometries of the blue naphthyl groups located at the “up” sides relative to the Rh1 and Rh2 centers (cf. top views from Rh1 and Rh2 in Figure 3A). These inequivalent chiral environments should lead to transition states with different geometries on both Rh centers in the stereo-determining C–C-bond-forming step to give a mixture of products with different enantioselectivities. Indeed, **2b** provided only moderate levels of enantioselectivity (67% ee) in the intramolecular C–H insertion of **11a** to give *trans*-lactone **12a** (Table 1, entry 10). Another noteworthy property of **2b** is the hydrogen bond formed between the carboxylate oxygen atom and the amide NH group (O⋯N distance: 2.71 (1) Å) in ligand II, which is shown by the dotted line in Figure 3A.

We have previously reported the solid-state stereostructure of the methoxycarbonyl-functionalized binaphthyl-type catalyst **2a** (Figure 3B).⁴ This complex forms a C₂-symmetric conformation in which the carbamate-substituted naphthyl rings of the ligands are oriented in an “up-up-down-down” conformation. However, this complex also contains unsymmetric chiral environments around Rh1 and Rh2, as shown by the different geometries of the blue naphthyl groups around the Rh1 and Rh2 centers. In this complex, two hydrogen bonds were found between the carboxylate oxygen atoms and the carbamate NH groups of the carboxylate ligands I and II located at the upper side of the complex relative to Rh1 (O⋯N distances: 2.974 (7) Å (ligand I); 2.962(7) Å (ligand II); dotted lines in Figure 3B). This complex also furnished *trans*-**12a** with unsatisfactory levels of enantioselectivity (55% ee) (Table 1, entry 9).

This was attributed to the unsymmetric chiral environments around the rhodium centers, similar to the case of **2b**. The crystal structures suggested that the unsymmetric stereostructures of **2a** and **2b** originate from the irregular angle of the naphthyl rings relative to the π -face of the carboxylate group via the rotation of the carboxylate C–C single bonds, as shown by the variation in their dihedral angles, i.e., ϕ C–C'–C''–O:

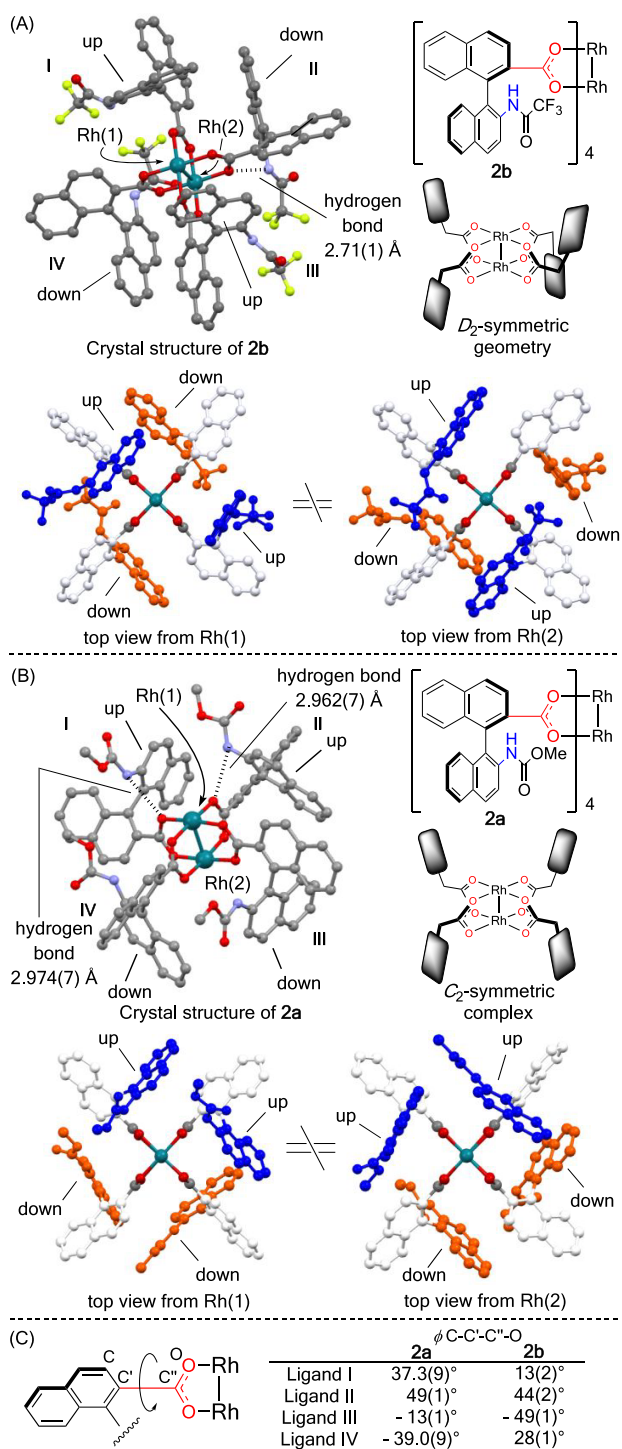
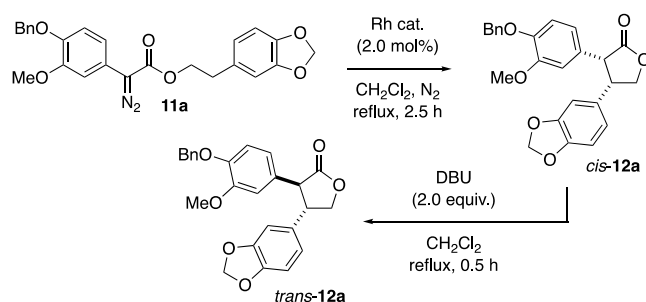


Figure 3. (A) Pseudo D_2 -symmetric structure of **2b**. (B) Pseudo C_2 -symmetric structure of **2a**. (C) Twist of the naphthyl rings relative to the π -face of the carboxylate group in **2a** and **2b** expressed as the dihedral angles around the carboxylate C–C bonds of ligands I–IV. In the crystal structures of **2a** and **2b**, the hydrogen atoms and solvent molecules coordinated at the axial positions are omitted for clarity. In the top views of the complexes, the pairs of amide-substituted naphthyl rings located at the upper and lower side relative to the indicated Rh center are shown in blue and orange, respectively.

–39.0(9)° to 49(1)° for ligands I–IV of complex **2a** and –49(1)° to 44(2)° for those of complex **2b** (Figure 3C).

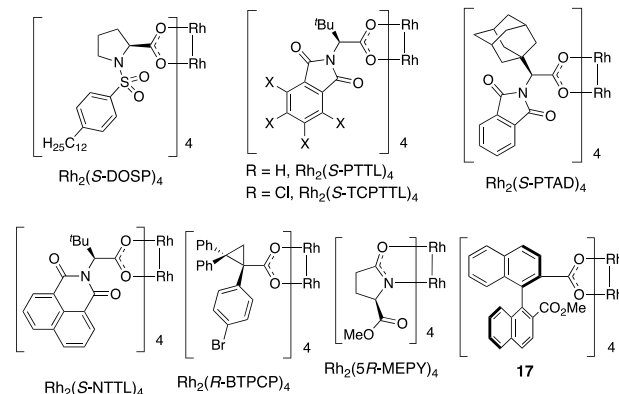
On the other hand, in sharp contrast to **2a** and **2b**, complex (S)-**10b** exhibits a well-ordered D_2 -symmetric stereostructure

Table 1. Survey of Dirhodium(II) Carboxylate Catalysts Tested in the Asymmetric Intramolecular C–H Insertion of **11a**^{a,h}



entry	Rh catalyst	<i>cis</i> - 12a (%) ^b	<i>trans</i> - 12a (%) ^c	ee (%) ^d of <i>trans</i> - 12a
1	Rh ₂ (S-DOSP) ₄	71	68	27
2	Rh ₂ (S-PTTL) ₄	64	64	–41
3	Rh ₂ (S-TCPTTL) ₄	80	80	–37
4	Rh ₂ (S-PTAD) ₄	61	60	–39
5	Rh ₂ (S-NTTL) ₄	69	68	–54
6	Rh ₂ (R-BTPCP) ₄	97	96	40
7	Rh ₂ (SR-MEPY) ₄ ^e	41	20	47
8	17	83	85	29
9	2a	65	60	55
10	2b	84	84	67
11	10a	81	81	70
12	(R)- 10b	96	95 ^f	95
13	(R)- 10b	95 ^f (95% ee) ^g		

^aStandard reaction conditions: **11a** (33.5 mg, 0.075 mmol, 1.0 equiv) in degassed CH₂Cl₂ (0.75 mL) was added over 1.5 h to 4.5 mL of a refluxing CH₂Cl₂ solution of the dirhodium(II) catalyst (1.5 μmol, 2.0 mol %); then, refluxing was continued for 1 h. ^bDetermined by integrating the ¹H NMR signals in the presence of the internal standard 1,3,5-trimethoxybenzene. ^cNMR yield over two steps. ^dDetermined by chiral HPLC analysis. ^e5 mol % of Rh₂(SR-MEPY)₄ was used. ^fIsolated yield. ^gEe (%) of isolated *cis*-**12a**.



in which the chiral environments around the Rh1 and Rh2 centers are almost identical (cf. the blue naphthothiophene rings in Figure 4A).^{20–22} Unlike in **2a** and **2b**, hydrogen bonding was not observed between the carboxylate oxygen atoms and the amide NH groups of the ligands. Instead, as expected, four chalcogen bonds, one between the sulfur atom of the naphthothiophene ring and the oxygen atom of the carboxylate group of each ligand, were observed in ligands I–IV and are shown as dotted lines in Figure 4A and exemplified by ligand III in Figure 4B. It should be noted here that all S···O

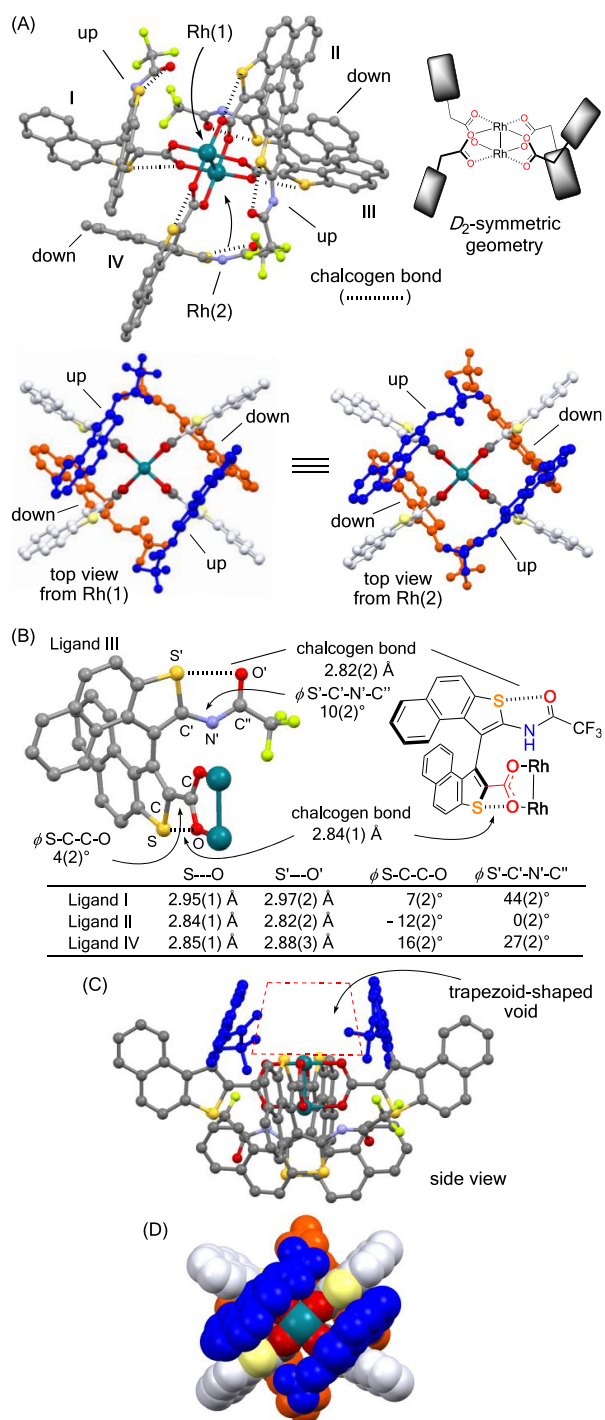


Figure 4. (A) D_2 -symmetric structure of (S)-10b. Hydrogen atoms and solvent molecules coordinated at the axial positions are omitted for clarity. In the top views of 10b, the pairs of amide-substituted naphthothiophene rings located at the upper and lower sides relative to the indicated Rh centers are shown in blue and orange, respectively. (B) Dihedral angles of S–C–C–O and S'–C'–N'–C'', as well as the S···O and S'···O' distances of each ligand; the locations of these angles and distances are illustrated using ligand III. (C) Side view of 10b. The blue amide-substituted naphthothiophene rings are located on the Rh(2) side. (D) Space-filling model of the top view from Rh(2).

distances (2.84 (1)–2.95 (1) Å) are shorter than the sum of the van der Waals radii (3.32 Å) of these atoms (Figure 4B). These chalcogen-bonding interactions could restrict the

flexibility around the carboxylate C–C bonds, thus resulting in a coplanar alignment of the carboxylate groups and the naphthothiophene π -systems in all the ligands (ϕ S–C–C–O $\leq \pm 16(2)^\circ$) (Figure 4B).

The defined conformations of the carboxylate moieties are crucial for the nearly perfect symmetric structure of 10b. Moreover, as expected, the coplanar geometry of the carboxylate and the naphthothiophene π -systems force the alternating naphthothiophene rings (blue) to tilt toward the Rh centers (cf. side view of the complex in Figure 4C). Due to the tilted aromatic rings in this D_2 -symmetric arrangement, trapezoidal chiral spaces are formed near each Rh center (the chiral space around Rh2 is indicated by a dotted line). Furthermore, chalcogen bonds between the carbonyl oxygen atom of the trifluoroacetamide moiety and a sulfur atom are also observed in all these ligands (S'···O' distances: 2.82(2)–2.97(2) Å) (Figure 4B). These chalcogen-bonding interactions make the trifluoroacetamide moieties form a five-membered 'heterocycle' parallel to the naphthothiophene rings (Figure 4B). The space-filling model of 10b revealed that a wide chiral cleft is formed by the fused cyclic systems of the naphthothiophene and trifluoroacetamide moieties (Figure 4D).

A natural bond orbital analysis of the crystal structure corroborated attractive S···O and S'···O' interactions due to the delocalization of lone pairs of electrons on the oxygen atoms into adjacent C–S σ^* orbitals in each ligand. The corresponding second order perturbation energies $E_{S\cdots O}$ (0.71 kcal/mol) and $E_{S'\cdots O'}$ (2.42 kcal/mol) in ligand III were determined by DFT calculations at the M06/6-31G*-[LANL2DZ] level of theory (Figure 5).²³

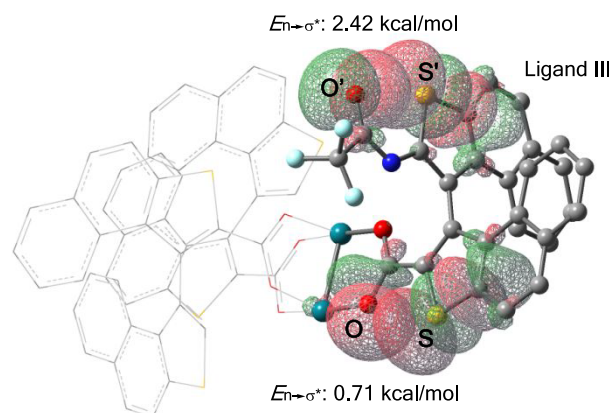
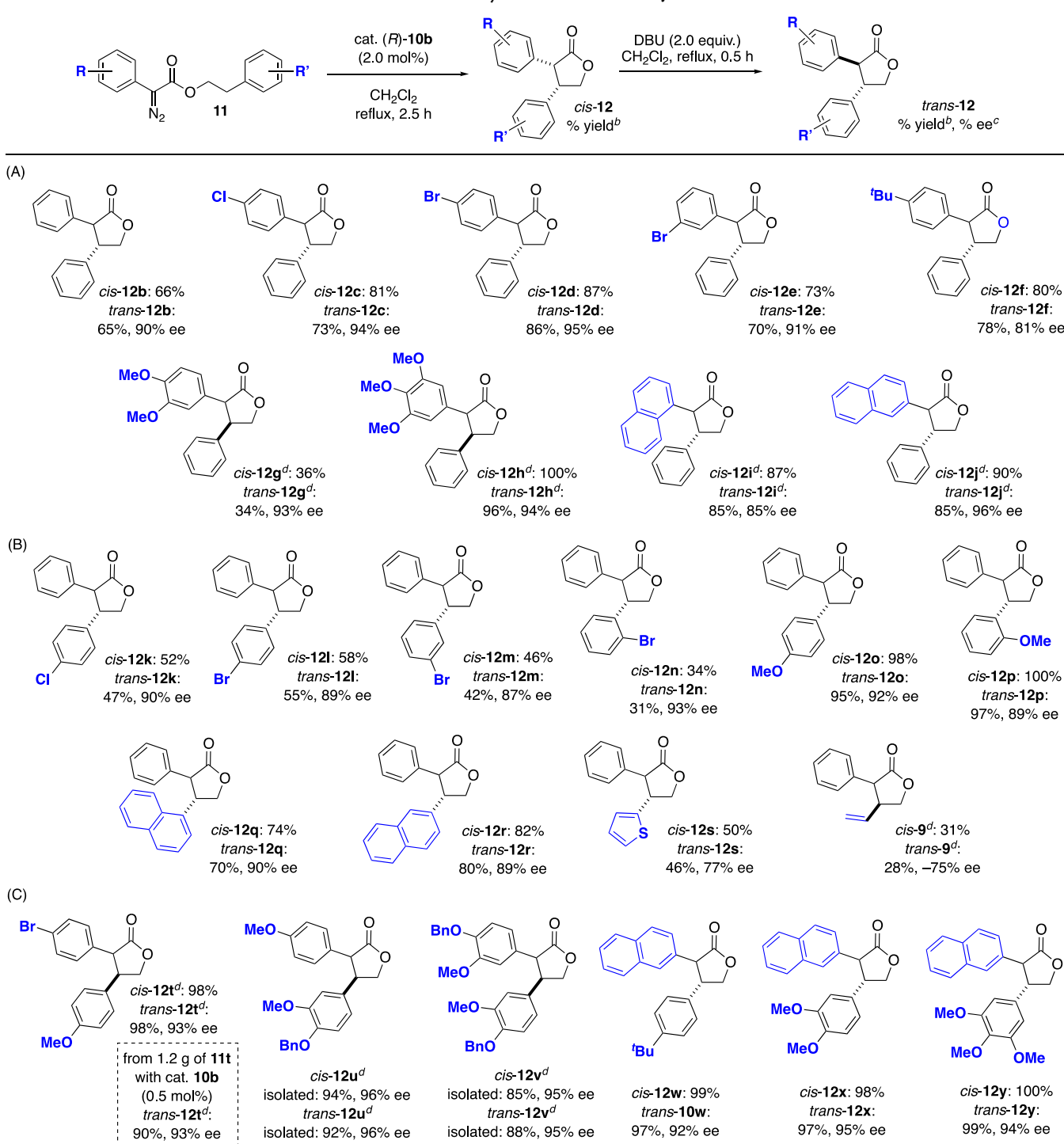


Figure 5. Natural bond orbital (NBO) overlap between the oxygen lone pair (n_O) and the antibonding orbital of the C–S bond (σ^*_{C-S}), together with the corresponding second order perturbation energies for ligand III in the crystal structure of (S)-10b.

These chalcogen-bonding interactions can be expected to contribute to the symmetric and defined structural properties of complex 10b. Having identified these promising structural features for asymmetric induction, we then moved on to examine intramolecular C–H insertion reactions using 10b.

Intramolecular C–H Insertion Reactions and Total Synthesis of Natural Products. The potential for asymmetric induction of each Rh complex was evaluated in the intramolecular C–H insertion reaction of 11a, as the product of this reaction provides ready access to cinnamomulide (13) (Table 1). After finding appropriate conditions by

Table 2. Intramolecular C–H Insertion to Give a Variety of *Cis*- and *Trans*- γ -Lactones^{a,b,c,d}

^aStandard reaction conditions: **11** (0.075 mmol, 1.0 equiv) in degassed CH₂Cl₂ (0.75 mL) was added over 1.5 h to 4.5 mL of a refluxing CH₂Cl₂ solution of **10b** (3.43 mg, 1.5 μ mol, 2.0 mol %); then, refluxing was continued for 1 h. ^bDetermined by integrating the ¹H NMR signals in the presence of the internal standard 1,3,5-trimethoxybenzene, except in the cases of **12u** and **12v**. ^cDetermined by chiral HPLC analysis. ^dCatalyst (S)-**10b** was used.

screening solvents and temperature (for details, see the Supporting Information), the intramolecular C–H insertion was examined in the presence of 2.0 mol % of the dirhodium(II) carboxylate complex in refluxing CH₂Cl₂. In all cases, *cis*-**12a** was obtained as the initial product in perfect diastereoselectivity (*cis:trans* > 99:1). However, although *cis*-**12a** was isolable, isomerization of *cis*-**12a** to *trans*-**12a** was

sometimes observed during the isolation. Therefore, epimerization to *trans*-**12a** was carried out by treatment with DBU after work up of the C–H insertion reaction. The chemical yield of *cis*-**12a** was determined using an internal standard, and the asymmetric induction was evaluated using the enantiomeric excess (ee) of *trans*-**12a**. The same ee value (95% ee) was measured for the isolated *cis*-**12a** and *trans*-**12a**,

demonstrating that no change in the optical purity occurred during the epimerization (entry 12 vs 13).

Initial trials of this reaction using several established catalysts, including $\text{Rh}_2(\text{S-DOSP})_4$,²⁴ $\text{Rh}_2(\text{S-PTTL})_4$,²⁵ $\text{Rh}_2(\text{S-TCPTTL})_4$,²⁶ $\text{Rh}_2(\text{S-PTAD})_4$,^{11c} $\text{Rh}_2(\text{S-NTTL})_4$,²⁷ $\text{Rh}_2(\text{R-BTPCP})_4$,²⁸ and $\text{Rh}_2(\text{SR-MEPY})_4$,²⁹ resulted in only low to medium levels of enantioselectivity (Table 1, entries 1–7). Moreover **2a**, **2b**, and binaphthyl-type catalyst **17**³⁰ were also tested. The use of **17** did not improve the ee (29%; entry 8). On the other hand, the pseudo C_2 -symmetric catalyst **2a** (Figure 3B) furnished *trans*-**12a** in 55% ee (entry 9), while pseudo D_2 -symmetric **2b** (Figure 3A) further improved the enantioselectivity to give *trans*-**12a** in 84% yield with 67% ee (entry 10). Although the stereoselectivity was still unsatisfactory, some improvement was observed using binaphthyl-type catalysts **2a** and **2b** instead of **17** (entries 9 and 10 vs entry 8).

While the different symmetries of the Rh complexes should significantly affect their performance with respect to enantioselectivity, the hydrogen bond formed between the carboxylate oxygen atom and the NH group of the amide and the carbamate substituents in **2a** and **2b** might also contribute to their increased stereoselectivity by acting as a conformational lock. A plausible explanation for the limited enantioselectivity of **2a** and **2b** might be the inequivalent chiral environments around their rhodium centers (Rh(1) and Rh(2)) (Figure 3A,B). These inequivalent chiral environments might lead to a decrease in enantioselectivity through transition states with different geometries in the stereo-determining C–C-bond-forming step. Thus, we examined the binaphthothiophene catalysts **10a** and **10b**.

Although methoxycarbonyl-functionalized **10a** furnished approximately the same level of enantioselectivity as **2b** (entry 11), the stereoselectivity was dramatically improved by the trifluoroacetamide-bearing (*R*)-**10b**, which gave *trans*-**12a** in 95% yield with 95% ee (entry 12). The initial product of the C–H insertion, *cis*-**12a**, was isolated in 95% yield with 95% ee under the same conditions (entry 13). These results confirm that **10b** is valuable for preparing both the corresponding *cis*- and *trans*-isomers in high diastereo- and enantioselectivity. As described below, the absolute configuration of *trans*-**12a** was determined to be 3*S*,4*S* by comparison of its optical rotation after transformation into cinnamomumolide (**13**).

The remarkable improvement in enantioselectivity using **10b** corroborates the importance of conformational control of the paddlewheel catalyst to give uniform and defined chiral environments around the catalytically active centers. Although **10a** provided only 70% ee, this value represents a significant increase compared to that achieved in the reaction using **2a** (55% ee), which contains the same substituents but no sulfur atoms (entry 9 vs entry 11). This improvement could be interpreted in terms of valuable control over the conformation of the ligands via chalcogen-bonding interactions.³¹ Furthermore, not only the stereoselectivity, but also the chemical yield of the product improved when **10b** was used. In this reaction, the dimerization of substrate **11a** tends to compete with the intramolecular C–H insertion to generate side products.³² The well-defined and rigid pockets formed by the naphthothiophene rings around the Rh centers of **10b** might also help to prevent these side reactions.

Having achieved satisfactory results using **10b**, we then explored its substrate scope. First, we tested substrates with a variety of α -aryl groups (Table 2A). The reactions of

unsubstituted **11b** and of **11c**–**11e**, which contain halogen groups at the *para*- or *meta*-positions, gave the corresponding products (*cis*- and *trans*-**12b**–**12e**) in good yield with excellent enantioselectivity (90–95% ee). The presence of a *t*-Bu group at the *para*-position of **11f** was still acceptable. On the other hand, a remarkable decrease in the chemical yield was observed in the reactions of *para*-methoxy-substituted **11g**, with 34% yield of the *trans*-isomer, although the enantioselectivity remained high. This could be due to the decreased electrophilicity of the rhodium-carbenoid intermediate formed by the α -phenyl moiety with an electron-donating *para*-methoxy group.

In contrast, **11h**, which contains two methoxy groups at its *meta*-positions, afforded *cis*-**12h** in high yield and 94% ee. The electron-withdrawing inductive effect of the *meta*-substituted methoxy groups may have contributed to this high yield. Naphthyl groups were also accepted and furnished *cis*- and *trans*-**12i** and **12j** in excellent yield, whereby **12j** showed the highest enantioselectivity of all products (96% ee).

The absolute configuration of *trans*-**12b** (3*S*,4*S*) was determined by comparison of its optical rotation to literature values³³ (cf. Supporting Information), and the absolute configuration of the other products was assigned in analogy.³⁴

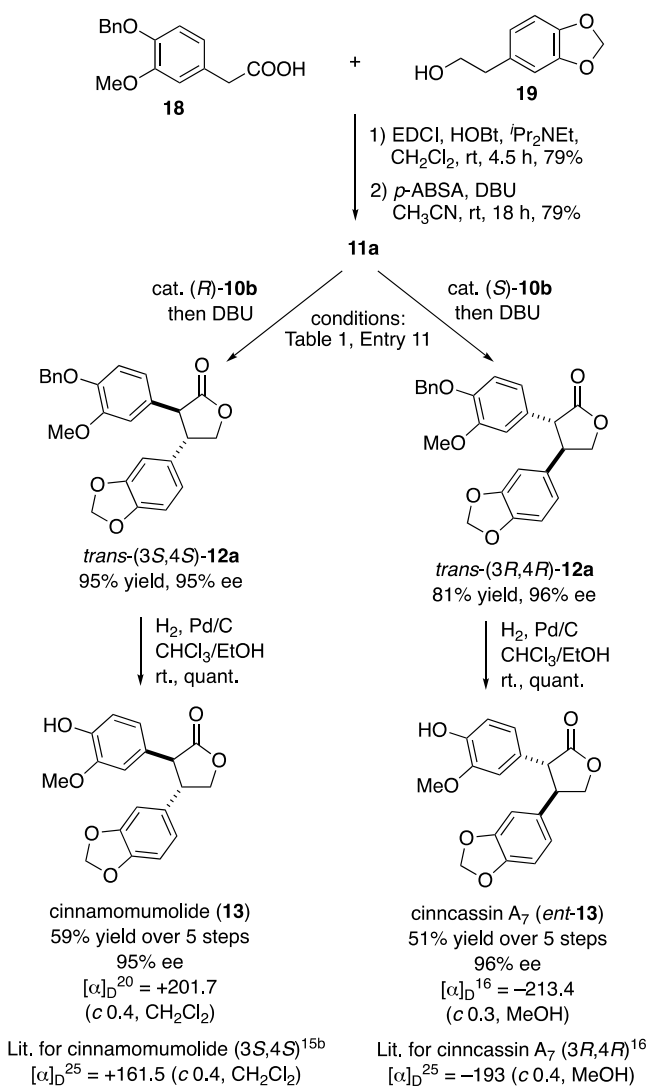
Subsequently, we tested the effect of the ester moiety (Table 2B). The reactions of the tested substrates generally proceeded with high enantioselectivity (87–93% ee for *trans*-**12k**–**12r**), although their chemical yield varies depending on the electronic nature of the aromatic rings. While the methoxy-functionalized substrates **11o** and **11p** afforded the products in excellent yield, substrates **11k**–**11n**, which bear electron-withdrawing groups, furnished the corresponding γ -lactones in moderate yield. This may have been due to the poorer stabilization of the positive charge at the benzylic position generated in the transition state for C–H insertion. Unfortunately, the C–H insertion of thiophene derivative **11s** and our previous substrate **8** did not produce promising results, providing the corresponding products *trans*-**12s** and *trans*-**9** in 46% yield and 77% ee as well as 28% yield and 75% ee, respectively.

Substrates bearing bromo, alkoxy, or 2-naphthyl groups on the α -aryl groups and electron-abundant aromatic groups in ester moieties generally furnished the corresponding products in high yield and enantioselectivity (Table 2C). It is noteworthy that substrate **11t** was reasonably converted on the gram scale at a reduced catalyst loading (0.5 mol %) to give *trans*-**12t** in 90% yield and 93% ee (cf. dashed box). In the case of **12u** and **12v**, the *cis*- γ -lactones were isolated to demonstrate the utility of this reaction for producing the *cis*-isomer.

Having established the substrate scope, we then applied the reaction to the total syntheses of naturally occurring γ -lactones. Cinnamomumolide (**13**), which exhibits a 3*S*,4*S* configuration, and its enantiomer, cinnassin A₇ (*ent*-**13**), which exhibits a 3*R*,4*R*-configuration, were readily prepared by removal of the benzyl group of the enantiomers *trans*-**12a** and *ent*-*trans*-**12a** (Scheme 2). Substrate **11a** was prepared from the commercially available compounds **18** and **19** in two steps. Therefore, cat. (*R*)- and (*S*)-**10b** enable the five-step stereoselective total syntheses of **13** and *ent*-**13** in 59 and 51% total yield, respectively. The absolute configurations of the prepared compounds were confirmed by comparison of their optical rotation with literature values.^{15b,16}

Furthermore, the total synthesis of cinnamomulactone (**14**) was achieved in five steps via the asymmetric intramolecular

Scheme 2. Asymmetric Syntheses of Cinnamomumolide (13) and Its Enantiomer Cinnacassin A7 (*ent*-13)



Scheme 3. Asymmetric Synthesis of Cinnamomulactone (14)

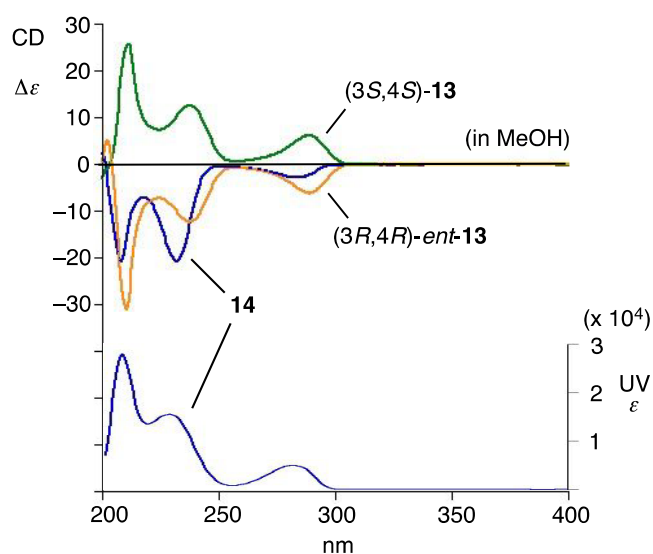
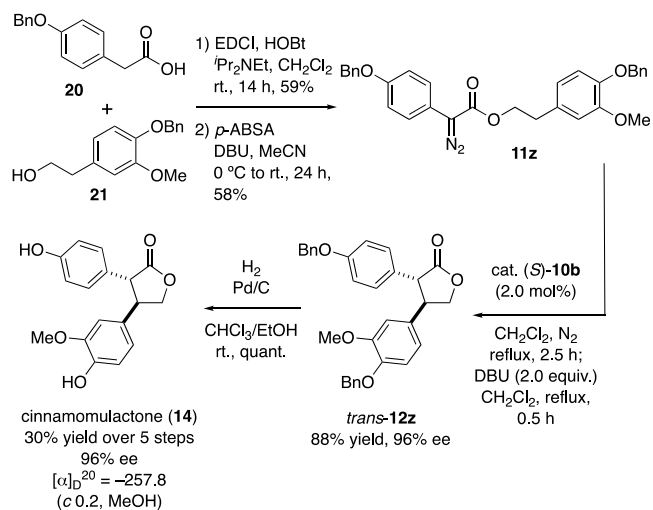


Figure 6. CD and UV spectra of 13, *ent*-13, and 14 in MeOH.

C–H insertion of 11z, which was prepared from commercially available 20 and 21, in the presence of (*S*)-10b, followed by deprotection of the benzyl groups of *trans*-12z (Scheme 3). Compound 14 was synthesized in the naturally occurring form, given that the optical rotation of synthesized 14 had the same sign as the isolated one from the natural source.¹⁷ However, the absolute configuration of 14 has not yet been determined, although the 3*R*,4*R* configuration was elucidated based on the opposite sign of the optical rotation ($[\alpha]_D^{25} = -193$ in CH₂Cl₂) relative to that of cinnamomumolide (13) ($[\alpha]_D^{25} = +161.5$ in CH₂Cl₂).¹⁷

To determine the absolute configuration of 14 unambiguously, the CD spectra of synthesized cinnamomumolide (3*S*,4*S*)-13, cinnacassin A₇ (3*R*,4*R*)-*ent*-13, and 14 were compared (Figure 6). Both 14 and *ent*-13 show negative Cotton effects at 270–300 nm, 230–250 nm, and 200–220 nm, which clearly indicate a 3*R*,4*R*-configuration of 14. The mirror image patterns of the CD spectra for 14 and (3*S*,4*S*)-13 also support the 3*R*,4*R*-configuration of 14. These asymmetric total syntheses aptly demonstrate the high applicability of cat. 10b for the preparation of optically active α,β -diaryl γ -lactones.

CONCLUSIONS

Chiral dirhodium(II) carboxylate complex 10b, which contains sulfur atoms in its fused cyclic system, was designed and synthesized. A single-crystal X-ray diffraction analysis indicated that the Rh centers in 10b are embedded in uniform and defined chiral environments that might arise from the presence of intramolecular chalcogen bonds. 10b demonstrated outstanding catalytic performance in diastereo- and enantioselective intramolecular C–H insertion reactions, as well as versatile synthetic utility in the concise asymmetric syntheses of the naturally occurring α,β -disubstituted γ -lactones such as 13, *ent*-13, and 14. These results demonstrate the importance of establishing conformational control in chiral paddlewheel complexes in order to achieve remarkable asymmetric induction. Furthermore, these results suggest that noncovalent interactions might play a significant role in controlling the conformation of catalysts that bear a rotatable bond near the catalytically active center. Further examination and applications of this concept of establishing conformational control via chalcogen-bonding interaction in asymmetric catalysts are currently in progress in our laboratories.

■ ASSOCIATED CONTENT

Supporting Information

The Supporting Information is available free of charge at <https://pubs.acs.org/doi/10.1021/acscatal.0c03689>.

General information; list of abbreviations; preparations of Rh(II) catalysts; preparations of substrates; optimization of reaction conditions for Rh(II)-catalyzed intramolecular C–H insertion; substrate scope for intramolecular C–H insertions; total syntheses of cinnamomumolide (**13**) and cinnassin A₇ (*ent*-**13**); total synthesis of cinnamomulactone (**14**); model to rationalize the stereoselectivity; and computational details (PDF)

HPLC analysis results for determination of the enantiomeric excess (PDF)

Spectroscopic data for all new compounds (PDF)

X-ray diffraction analysis results for **2a** (CIF)

X-ray diffraction analysis results for **2b** (CIF)

X-ray diffraction analysis results for (*S*)-**10b** (CIF)

■ AUTHOR INFORMATION

Corresponding Author

Takumi Furuta – Department of Pharmaceutical Chemistry, Kyoto Pharmaceutical University, Yamashina-ku, Kyoto 607-8414, Japan; orcid.org/0000-0003-1037-9715; Email: furuta@mb.kyoto-phu.ac.jp

Authors

Takuya Murai – Department of Pharmaceutical Chemistry, Kyoto Pharmaceutical University, Yamashina-ku, Kyoto 607-8414, Japan

Wenjie Lu – Institute for Chemical Research, Kyoto University, Uji, Kyoto 611-0011, Japan

Toshifumi Kuribayashi – Institute for Chemical Research, Kyoto University, Uji, Kyoto 611-0011, Japan

Kazuhiro Morisaki – Institute for Chemical Research, Kyoto University, Uji, Kyoto 611-0011, Japan

Yoshihiro Ueda – Institute for Chemical Research, Kyoto University, Uji, Kyoto 611-0011, Japan; orcid.org/0000-0002-5485-2722

Shohei Hamada – Department of Pharmaceutical Chemistry, Kyoto Pharmaceutical University, Yamashina-ku, Kyoto 607-8414, Japan

Yusuke Kobayashi – Department of Pharmaceutical Chemistry, Kyoto Pharmaceutical University, Yamashina-ku, Kyoto 607-8414, Japan; orcid.org/0000-0003-3074-7378

Takahiro Sasamori – Graduate School of Natural Sciences, Nagoya City University, Nagoya, Aichi 467-8501, Japan; orcid.org/0000-0001-5410-8488

Norihiro Tokitoh – Institute for Chemical Research, Kyoto University, Uji, Kyoto 611-0011, Japan; orcid.org/0000-0003-1083-7245

Takeo Kawabata – Institute for Chemical Research, Kyoto University, Uji, Kyoto 611-0011, Japan; orcid.org/0000-0002-9959-0420

Complete contact information is available at: <https://pubs.acs.org/doi/10.1021/acscatal.0c03689>

Author Contributions

The manuscript was collated by contributions from all authors.

Notes

The authors declare no competing financial interest.

■ ACKNOWLEDGMENTS

This work was financially supported by a Grant-in-Aid for Scientific Research (C) (26460007) and Scientific Research (B) (18H02554).

■ REFERENCES

- (1) (a) Davies, H. M. L.; Beckwith, R. E. J. Catalytic Enantioselective C–H Activation by Means of Metal–Carbenoid-Induced C–H Insertion. *Chem. Rev.* **2003**, *103*, 2861–2904. For reviews, see (b) Slattery, C. N.; Ford, A.; Maguire, A. R. Catalytic Asymmetric C–H Insertion Reactions of α -Diazocarbonyl Compounds. *Tetrahedron* **2010**, *66*, 6681–6705. (c) Doyle, M. P.; Duffy, R.; Ratnikov, M.; Zhou, L. Catalytic Carbene Insertion into C–H Bonds. *Chem. Rev.* **2010**, *110*, 704–724. (d) Doyle, M. P.; Liu, Y.; Ratnikov, M. Catalytic, Asymmetric, Intramolecular Carbon–Hydrogen Insertion. *Org. React.* **2013**, *80*, 1–132. (e) Ford, A.; Miel, H.; Ring, A.; Slattery, C. N.; Maguire, A. R.; McKerverve, M. A. Modern Organic Synthesis with α -Diazocarbonyl Compounds. *Chem. Rev.* **2015**, *115*, 9981–10080. (f) Davies, H. M. L.; Liao, K. Dirhodium Tetracarboxylates as Catalysts for Selective Intramolecular C–H Insertion. *Nat. Rev. Chem.* **2019**, *3*, 347–360. (g) Fu, J.; Ren, Z.; Bacsá, J.; Musaev, D. G.; Davies, H. M. L. Desymmetrization of Cyclohexanes by Site- and Stereoselective C–H Functionalization. *Nature* **2018**, *564*, 395–399. For recent examples, see (h) Garlets, Z. J.; Wertz, B. D.; Liu, W.; Voight, E. A.; Davies, H. M. L. Regio- and Stereoselective Rhodium(II)-Catalyzed C–H Functionalization of Cyclobutanes. *Chem* **2020**, *6*, 304–313. (i) Garlets, Z. J.; Sanders, J. N.; Malik, H.; Gampe, C.; Houk, K. N.; Davies, H. M. L. Enantioselective C–H Functionalization of Bicyclo[1.1.1]pentanes. *Nat. Catal.* **2020**, *3*, 351–357. (j) Wei, B.; Sharland, J. C.; Lin, P.; Wilkerson-Hill, S. M.; Fullilove, F. A.; McKinnon, S.; Blackmond, D. G.; Davies, H. M. L. In Situ Kinetic Studies of Rh(II)-Catalyzed Asymmetric Cyclopropanation with Low Catalyst Loadings. *ACS Catal.* **2020**, *10*, 1161–1170. (k) Caló, F. P.; Fürstner, A. A Heteroleptic Dirhodium Catalyst for Asymmetric Cyclopropanation with α -Stannyl α -Diazoacetate. “Stereoentensive” Stille Coupling with Formation of Chiral Quaternary Carbon Centers. *Angew. Chem., Int. Ed.* **2020**, *59*, 13900–13907.
- (2) Hansen, J.; Davies, H. M. L. High Symmetry Dirhodium(II) Paddlewheel Complexes as Chiral Catalysts. *Coord. Chem. Rev.* **2008**, *252*, 545–555.
- (3) Furuta, T.; Yamamoto, J.; Kitamura, Y.; Hashimoto, A.; Masu, H.; Azumaya, I.; Kan, T.; Kawabata, T. Synthesis of Axially Chiral Amino Acid and Amino Alcohols via Additive-Ligand-Free Pd-Catalyzed Domino Coupling Reaction and Subsequent Transformations of the Product Amidoaza[5]helicene. *J. Org. Chem.* **2010**, *75*, 7010–7013.
- (4) Lu, W.-J.; Xu, P.; Murai, T.; Sasamori, T.; Tokitoh, N.; Kawabata, T.; Furuta, T. Asymmetric Intramolecular C–H Insertion Promoted by Dirhodium(II) Carboxylate Catalyst Bearing Axially Chiral Amino Acid Derivatives. *Synlett* **2017**, *28*, 679–683.
- (5) Murai, T.; Xing, Y.; Kuribayashi, T.; Lu, W.; Guo, J.-D.; Yella, R.; Hamada, S.; Sasamori, T.; Tokitoh, N.; Kawabata, T.; Furuta, T. Synthesis and Structural Properties of Axially Chiral Binaphthothiophene Dicarboxylic Acid. *Chem. Pharm. Bull.* **2018**, *66*, 1203–1206.
- (6) Hamada, S.; Wang, S.; Murai, T.; Xing, Y.; Inoue, T.; Ueda, Y.; Sasamori, T.; Kawabata, T.; Furuta, T. Synthesis of Axially Chiral Binaphthothiophene δ -Amino Acid Derivatives Bearing Chalcogen Bonds. *Heterocycles* **2020**, *75*, 7010–7013.
- (7) (a) Nagao, Y.; Hirata, T.; Goto, S.; Sano, S.; Kakehi, A.; Iizuka, K.; Shiro, M. Intramolecular Nonbonded S...O Interaction Recognized in (Acylimino)thiadiazoline Derivatives as Angiotensin II Receptor Antagonists and Related Compounds. *J. Am. Chem. Soc.* **1998**, *120*, 3104–3110. (b) Iwaoka, M.; Takemoto, S.; Tomoda, S. Statistical and Theoretical Investigations on the Directionality of Nonbonded S...O Interactions. Implications for Molecular Design

and Protein Engineering. *J. Am. Chem. Soc.* **2002**, *124*, 10613–10620. (c) Tsuzuki, S.; Sato, N. Origin of Attraction in Chalcogen–Nitrogen Interaction of 1,2,5-Chalcogenadiazole Dimers. *J. Phys. Chem. B* **2013**, *117*, 6849–6855. (d) Beno, B. R.; Yeung, K.-S.; Bartberger, M. D.; Pennington, L. D.; Meanwell, N. A. A Survey of the Role of Noncovalent Sulfur Interactions in Drug Design. *J. Med. Chem.* **2015**, *58*, 4383–4438. (e) Pascoe, D. J.; Ling, K. B.; Cockroft, S. L. The Origin of Chalcogen-Bonding Interactions. *J. Am. Chem. Soc.* **2017**, *139*, 15160–15167. (f) Huang, H.; Yang, L.; Facchetti, A.; Marks, T. J. Organic and Polymeric Semiconductors Enhanced by Noncovalent Conformational Locks. *Chem. Rev.* **2017**, *117*, 10291–10318. (g) Mahmudov, K. T.; Kopylovich, M. N.; Guedes da Silva, M. F. C.; Pombeiro, A. J. L. Chalcogen Bonding in Synthesis, Catalysis and Design of Materials. *Dalton Trans.* **2017**, *46*, 10121–10138. (h) Noh, J.; Jung, A.; Koo, D. G.; Kim, G.; Choi, K. S.; Park, J.; Shin, T. J.; Yang, C.; Park, J. Thienoisindigo-Based Semiconductor Nanowires Assembled with 2-Bromobenzaldehyde via Both Halogen and Chalcogen Bonding. *Sci. Rep.* **2018**, *8*, 14448. (i) Zhou, B.; Gabbai, F. P. Redox-Controlled Chalcogen-Bonding at Tellurium: Impact on Lewis Acidity and Chloride Anion Transport Properties. *Chem. Sci.* **2020**, *11*, 7495–7500. (j) Wirth, T. Organoselenium Chemistry in Stereoselective Reactions. *Angew. Chem., Int. Ed.* **2000**, *39*, 3740–3749. Chalcogen bonding interactions have been employed for inducing conformational rigidity into chiral organoselenium compounds. For reviews, see (k) Mukherjee, A. J.; Zade, S. S.; Singh, H. B.; Sunoj, R. B. Organoselenium Chemistry: Role of Intramolecular Interactions. *Chem. Rev.* **2010**, *110*, 4357–4416.

(8) (a) Benz, S.; López-Andarias, J.; Mareda, J.; Sakai, N.; Matile, S. Catalysis with Chalcogen Bonds. *Angew. Chem., Int. Ed.* **2017**, *56*, 812–815. (b) Benz, S.; Mareda, J.; Besnard, C.; Sakai, N.; Matile, S. Catalysis with Chalcogen Bonds: Neutral Benzodiselenazole Scaffolds with High-Precision Selenium Donors of Variable Strength. *Chem. Sci.* **2017**, *8*, 8164–8169. (c) Wang, W.; Zhu, H.; Liu, S.; Zhao, Z.; Zhang, L.; Hao, J.; Wang, Y. Chalcogen–Chalcogen Bonding Catalysis Enables Assembly of Discrete Molecules. *J. Am. Chem. Soc.* **2019**, *141*, 9175–9179. (d) Bamberger, J.; Ostler, F.; Mancheño, O. G. Frontiers in Halogen and Chalcogen-Bond Donor Organocatalysis. *ChemCatChem* **2019**, *11*, 5198–5211. (e) Vogel, L.; Wöchner, P.; Huber, S. M. Chalcogen Bonding: An Overview. *Angew. Chem., Int. Ed.* **2019**, *58*, 1880–1891. (f) Strakova, K.; Assies, L.; Goujon, A.; Piazzolla, F.; Humeniuk, H. V.; Matile, S. Dithienothiophenes at Work: Access to Mechanosensitive Fluorescent Probes, Chalcogen-Bonding Catalysis, and Beyond. *Chem. Rev.* **2019**, *119*, 10977–11005. (g) Young, C. M.; Elmi, A.; Pascoe, D. J.; Morris, R. K.; McLaughlin, C.; Woods, A. M.; Frost, A. B.; de la Houpliere, A.; Ling, K. B.; Smith, T. K.; Slawin, A. M. Z.; Willoughby, P. H.; Cockroft, S. L.; Smith, A. D. The Importance of 1,5-Oxygen-Chalcogen Interactions in Enantioselective Isochalcogenourea Catalysis. *Angew. Chem., Int. Ed.* **2020**, *59*, 3705–3710. (h) Wang, W.; Zhu, H.; Feng, L.; Yu, Q.; Hao, J.; Zhu, R.; Wang, Y. Dual Chalcogen–Chalcogen Bonding Catalysis. *J. Am. Chem. Soc.* **2020**, *142*, 3117–3124.

(9) (a) Riwer, L.-J.; Trapp, N.; Root, K.; Zenobi, R.; Diederich, F. Supramolecular Capsules: Strong Versus Weak Chalcogen Bonding. *Angew. Chem., Int. Ed.* **2018**, *57*, 17259–17264. (b) Rahman, F.-J.; Tzeli, D.; Petsalakis, I. D.; Theodorakopoulos, G.; Ballester, P.; Rebek, J., Jr.; Yu, Y. Chalcogen Bonding and Hydrophobic Effects Force Molecules into Small Spaces. *J. Am. Chem. Soc.* **2020**, *142*, 5876–5883.

(10) Halogen-bonding interactions were found in the dirhodium carboxylate complexes $\text{Rh}_2(\text{S-TCPTTL})_4$ and its bromo derivative. These interactions are considered to work as a conformational lock for their C_4 -symmetric structures. For details, see: (a) Goto, T.; Takeda, K.; Shimada, N.; Nambu, H.; Anada, M.; Shiro, M.; Ando, K.; Hashimoto, S. Highly Enantioselective Cyclopropanation Reaction of 1-Alkynes with α -Alkyl- α -Diazooesters Catalyzed by Dirhodium(II) Carboxylates. *Angew. Chem., Int. Ed.* **2011**, *50*, 6803–6808. (b) Lindsay, V. N. G.; Lin, W.; Charette, A. B. Experimental Evidence for the All-Up Reactive Conformation of Chiral Rhodium-

(II) Carboxylate Catalysts: Enantioselective Synthesis of *cis*-Cyclopropane α -Amino Acid. *J. Am. Chem. Soc.* **2009**, *131*, 16383–16385.

(11) For examples of stereoselective intramolecular C–H insertions, see: (a) Davies, H. M. L.; Grazini, M. V. A.; Aouad, E. Asymmetric Intramolecular C–H Insertions of Aryldiazoacetates. *Org. Lett.* **2001**, *3*, 1475–1477. (b) Saito, H.; Oishi, H.; Kitagaki, S.; Nakamura, S.; Anada, M.; Hashimoto, S. Enantio- and Diastereoselective Synthesis of *cis*-2-Aryl-3-methoxycarbonyl-2,3-dihydrobenzofurans via the Rh(II)-Catalyzed C–H Insertion Process. *Org. Lett.* **2002**, *4*, 3887–3890. (c) Reddy, R. P.; Lee, G. H.; Davies, H. M. L. Dirhodium Tetracarboxylate Derived from Adamantylglycine as a Chiral Catalyst for Carbenoid Reactions. *Org. Lett.* **2006**, *8*, 3437–3440. (d) Koizumi, Y.; Kobayashi, H.; Wakimoto, T.; Furuta, T.; Fukuyama, T.; Kan, T. Total Synthesis of (–)-Serotobenine. *J. Am. Chem. Soc.* **2008**, *130*, 16854–16855. (e) Natori, Y.; Tsutsui, H.; Sato, N.; Nakamura, S.; Nambu, H.; Shiro, M.; Hashimoto, S. Asymmetric Synthesis of Neolignans (–)-*epi*-Conocarpan and (+)-Conocarpan via Rh(II)-Catalyzed C–H Insertion Process and Revision of the Absolute Configuration of (–)-*epi*-Conocarpan. *J. Org. Chem.* **2009**, *74*, 4418–4421. (f) Miyazawa, T.; Minami, K.; Ito, M.; Anada, M.; Matsunaga, S.; Hashimoto, S. Enantio- and Diastereoselective Desymmetrization of α -Alkyl- α -Diazooesters by Dirhodium(II)-Catalyzed Intramolecular C–H Insertion. *Tetrahedron* **2016**, *72*, 3939–3947. (g) Miyazawa, T.; Imai, K.; Ito, M.; Takeda, K.; Anada, M.; Matsunaga, S.; Hashimoto, S. Diastereo- and Enantioselective Construction of 6,7-Dioxabicyclo[2.2.1]heptane Derivatives by a Dirhodium(II)-Catalyzed Intramolecular C–H Insertion Reaction. *Heterocycles* **2017**, *95*, 1211–1229.

(12) Enantioselective intramolecular C–H insertions of α -aryl- α -diazoacetates, see: (a) Doyle, M. P.; May, E. J. Enantioselective β -Lactone Formation from Phenyl diazoacetates via Catalytic Intramolecular Carbon–Hydrogen Insertion. *Synlett* **2001**, *2001*, 967–969. (b) Doyle, M. P.; Davies, S. B.; May, E. J. High Selectivity from Configurational Match/Mismatch in Carbon–Hydrogen Insertion Reactions of Steroidal Diazoacetates Catalyzed by Chiral Dirhodium(II) Carboxamidates. *J. Org. Chem.* **2001**, *66*, 8112–8119. Diastereoselective inside-type intramolecular C–H insertions of α -aryl- α -diazoacetates, see (c) Villalobos, M. N.; Wood, J. L. Spirolactone Syntheses through a Rhodium-Catalyzed Intramolecular C–H Insertion Reaction: Model Studies towards the Synthesis of Syringolides. *Tetrahedron Lett.* **2009**, *50*, 6450–6453.

(13) Fu, L.; Wang, H.; Davies, H. M. L. Role of *Ortho*-Substituents on Rhodium-Catalyzed Asymmetric Synthesis of β -Lactones by Intramolecular C–H Insertions of Aryldiazoacetates. *Org. Lett.* **2014**, *16*, 3036–3039.

(14) (a) He, S.; Zeng, K.-W.; Jiang, Y.; Tu, P.-F. Nitric Oxide Inhibitory Constituents from the Barks of *Cinnamomum cassia*. *Fitoterapia* **2016**, *112*, 153–160. (b) Itokawa, H.; Ibraheim, Z. Z.; Qiao, Y. F.; Takeya, K. Anthraquinone, Naphthohydroquinones and naphthohydroquinone Dimers from *Rubia cordifolia* and Their Cytotoxic Activity. *Chem. Pharm. Bull.* **1993**, *41*, 1869–1872. (c) Lumb, J.-P.; Choong, K. C.; Trauner, D. *ortho*-Quinone Methides from *para*-Quinones: Total Synthesis of Rubioncolin B. *J. Am. Chem. Soc.* **2008**, *130*, 9230–9231. (d) Ma, S.-S.; Mei, W.-L.; Guo, Z.-K.; Liu, S.-B.; Zhao, Y.-X.; Yang, D.-L.; Zeng, Y.-B.; Jiang, B.; Dai, H.-F. Two New Types of Bisindole Alkaloid from *Trigonostemon lutescens*. *Org. Lett.* **2013**, *15*, 1492–1495.

(15) For the isolation of **13**, see: (a) Liu, C.; Zhong, S.-M.; Chen, R.-Y.; Wu, Y.; Zhu, X.-J. Two New Compounds from the Dried Tender Stems of *Cinnamomum cassia*. *J. Asian Nat. Prod. Res.* **2009**, *11*, 845–849. For the asymmetric total synthesis of **13**, see: (b) Chen, J.-P.; Ding, C.-H.; Liu, W.; Hou, X.-L.; Dai, L.-X. Palladium-Catalyzed Regio-, Diastereo-, and Enantioselective Allylic Alkylation of Acylsilanes with Monosubstituted Allyl Substrates. *J. Am. Chem. Soc.* **2010**, *132*, 15493–15495.

(16) Liu, X.; Fu, J.; Yao, X.-J.; Yang, J.; Liu, L.; Xie, T.-G.; Jiang, P.-C.; Jiang, Z.-H.; Zhu, G.-Y. Phenolic Constituents Isolated from the Twigs of *Cinnamomum cassia* and Their Potential Neuroprotective Effects. *J. Nat. Prod.* **2018**, *81*, 1333–1342.

(17) Kim, G. J.; Lee, J. Y.; Choi, H. G.; Kim, S. Y.; Kim, E.; Shim, S. H.; Nam, J.-W.; Kim, S.-H.; Choi, H. Cinnamomulactone, a New Butyrolactone from the Twigs of *Cinnamomum cassia* and its Inhibitory Activity of Matrix Metalloproteinases. *Arch. Pharm. Res.* **2017**, *40*, 304–310.

(18) The X-ray data for **2b** has been deposited at the Cambridge Crystallographic Data Center under reference number CCDC 1839246.

(19) For a typical example of a D_2 -symmetric dirhodium(II) tetracarboxylate catalyst, see: Liao, K.; Negretti, S.; Musaev, D. G.; Bacsá, J.; Davies, H. M. L. Site-Selective and Stereoselective Functionalization of Unactivated C–H Bonds. *Nature* **2016**, *533*, 230–234.

(20) The X-ray data for **10b** has been deposited at the Cambridge Crystallographic Data Center under reference number CCDC 1837271.

(21) DFT calculations on (*S*)-**10b** indicated that the D_2 (up-down-up-down)-symmetric structure was more stable than the other possible C_1 (up-up-up-down)-, C_2 (up-up-down-down)-, and C_4 (all up)-symmetric structures. For details, see the Supporting Information.

(22) It is noteworthy that the molecular symmetry changes from C_2 to D_2 from **2a** to **2b** and **10b**. At present, we do not have a clear explanation for this change in symmetry. However, in the cases of **2b** and **10b**, close contacts between the fluorine atoms of the trifluoroacetamide groups on different ligands were observed (cf. Supporting Information). These contacts might also act as conformational locks in the D_2 -symmetric structures. An example of fluorine-fluorine close contact, see: Rusek, M.; Kwasna, K.; Budzianowski, A.; Katrusiak, A. Fluorine...Fluorine Interactions in a High-Pressure Layered Phase of Perfluorobenzene. *J. Phys. Chem. C* **2020**, *124*, 99–106.

(23) For the second order perturbation energies of the S...O and S'...O' interactions in ligand I, II, and IV, see the Supporting Information.

(24) Davies, H. M. L.; Bruzinski, P. R.; Lake, D. H.; Kong, N.; Fall, M. J. Asymmetric Cyclopropanations by Rhodium(II) *N*-(Arylsulfonyl)prolinate Catalyzed Decomposition of Vinyl diazomethanes in the Presence of Alkenes. Practical Enantioselective Synthesis of the Four Stereoisomers of 2-Phenylcyclopropan-1-amino Acid. *J. Am. Chem. Soc.* **1996**, *118*, 6897–6907.

(25) Watanabe, N.; Ogawa, Y.; Ohtake, S.; Ikegami, S.; Hashimoto, S.-I. Dirhodium(II) Tetrakis[*N*-phthaloyl-(*S*)-*tert*-leucinate]: A Notable Catalyst for Enantiotopically Selective Aromatic Substitution Reactions of α -Diazocarbonyl Compounds. Amidation of C–H Bonds. *Synlett* **1996**, 85–86.

(26) Yamawaki, M.; Tsutsui, H.; Kitagaki, S.; Anada, M.; Hashimoto, S. Dirhodium(II) Tetrakis[*N*-tetrachlorophthaloyl-(*S*)-*tert*-leucinate]: a New Chiral Rh(II) Catalyst for Enantioselective Amidation of C–H Bonds. *Tetrahedron Lett.* **2002**, *43*, 9561–9564.

(27) Müller, P.; Allenbach, Y.; Robert, E. Rhodium(II)-Catalyzed Olefin Cyclopropanation with the Phenyliodonium Ylide Derived from Meldrum's Acid. *Tetrahedron: Asymmetry* **2003**, *14*, 779–785.

(28) Qin, C.; Boyarskikh, V.; Hansen, J. H.; Hardcastle, K. I.; Musaev, D. G.; Davies, H. M. L. D_2 -Symmetric Dirhodium Catalyst Derived from a 1,2,2-Triarylcyclopropanecarboxylate Ligand: Design, Synthesis and Application. *J. Am. Chem. Soc.* **2011**, *133*, 19198–19204.

(29) Doyle, M. P.; Bagheri, V.; Wandless, T. J.; Harn, N. K.; Brinker, D. A.; Eagle, C. T.; Loh, K. L. Exceptionally High Trans (Anti) Stereoselectivity in Catalytic Cyclopropanation Reactions. *J. Am. Chem. Soc.* **1990**, *112*, 1906–1912.

(30) Hikichi, K.; Kitagaki, S.; Anada, M.; Nakamura, S.; Nakajima, M.; Shiro, M.; Hashimoto, S. Synthesis and Evaluation of Novel Dirhodium(II) Carboxylate Catalysts with Atropisomeric Biaryl Backbone. *Heterocycles* **2003**, *12*, 4391–4401.

(31) The structure of binaphthofuran analog of cat. **10b** was also calculated by DFT method for evaluation of the contribution of the chalcogen-bonding interactions in cat. **10b**. The optimized structure of the binaphthofuran complex, which would lack the strong chalcogen

bonding interactions, showed unsymmetrical structural property. This result supported the contribution of the chalcogen-bonding interactions for symmetric and defined structure of cat. **10b**, as well as its high level of stereoselectivity. The optimized structures of binaphthofuran analog and cat. **10b** by the DFT calculation, see the Supporting Information.

(32) The *E/Z*-mixture of the olefin dimer of **11a** and the hydroxylated product were generated as the main side products. For the chemical yields of these compounds, see the Supporting Information.

(33) Berova, N. D.; Kurtev, B. J. Absolute Configurations of Some 1,2-Diphenylethane Derivatives. *Tetrahedron* **1969**, *25*, 2301–2311.

(34) The model to rationalize the stereoselectivity, see the Supporting Information.